

## Deactivation of Fe-K commercial catalysts during ethylbenzene dehydrogenation and novel method for their regeneration

M.Khatamian<sup>1</sup>, M.Ghadiri<sup>1,2\*</sup>, M.Haghighi<sup>3</sup>

<sup>1</sup>Inorganic Chemistry Department, Faculty of Chemistry, University of Tabriz, C.P. 51664, Tabriz, (IRAN)

<sup>2</sup>Chemical Engineering Department, Urmia University of Technology (UUT), Urmia 57155-419, (IRAN)

<sup>3</sup>Reactor and Catalysis Research Center (RCRC), Chemical Engineering Department, Sahand University of Technology, P.O.Box 51335-1996, Sahand New Town, Tabriz, (IRAN)

E-mail: m.ghadiri@uut.ac.ir

### ABSTRACT

Deactivation of Fe-K commercial catalyst has been studied during the ethylbenzene dehydrogenation to styrene. After using the catalyst for two years, a long-term reaction test led to 15% reduction in the styrene selectivity. For the activation of these catalysts, oxidants like N<sub>2</sub>O, CO<sub>2</sub>, air, steam and mixtures of these components have been examined. Fresh, used and regenerated catalysts were characterized by X-ray diffraction (XRD), scanning electron microscope (SEM), BET measurement, ICP elemental analysis and hydrogen temperature-programmed reduction (H<sub>2</sub>-TPR). Catalytic dehydrogenation of ethylbenzene to produce styrene was investigated using fresh, used and regenerated catalysts at 660°C and atmospheric pressure in the presence of steam. Results have demonstrated that high tendency of N<sub>2</sub>O to increase the Fe<sub>2</sub>O<sub>3</sub> active phase and regain the oxidation state of iron. © 2014 Trade Science Inc. - INDIA

### KEYWORDS

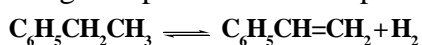
Fe-K catalysts;  
Styrene;  
Ethylbenzene;  
Dehydrogenation;  
Regeneration;  
Deactivation.

### INTRODUCTION

The catalytic dehydrogenation of ethylbenzene to styrene is of increasing interest due to the growing demand for styrene. This valued product is an important raw material for producing acrylonitrile-butadiene-styrene resins, expandable styrene-butadiene latex, and a variety of synthetic polymers<sup>[1,2]</sup>.

Catalytic dehydrogenation of ethylbenzene is a well-known reaction at industrial stage, which is carried out over potassium-promoted iron oxide catalysts in the presence of superheated steam. Steam does not participate in the reaction but increases the activity and selectivity of the catalyst<sup>[3,4]</sup>. This reaction is endothermic (reaction 1), and high conversions are obtained only

at high temperatures and low pressures:



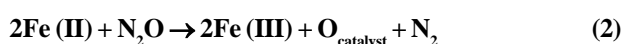
$$\Delta H = 117.6 \text{ kJ/mol} \quad (1)$$

Reaction (1) can also promote Fe<sup>3+</sup> reduction, as verified by analyzing the catalysts after the reaction process<sup>[1]</sup>. Furthermore, it has been found that the potassium ferrites containing mainly Fe<sup>3+</sup> ions show higher activity compared to the one with Fe<sup>2+</sup> sites. The loss of activity of commercial catalysts during the dehydrogenation reaction has been already discussed and interpreted as potassium loss and auto-reduction of Fe<sup>3+</sup> to Fe<sup>2+</sup><sup>[1,5]</sup>.

The Fe<sup>3+</sup> reduction can promote the formation of FeO, which is catalytically inactive<sup>[6,7]</sup>, or the formation

of  $\text{Fe}_3\text{O}_4$ , which exhibits only a minor catalytic activity<sup>[11,8]</sup> in the dehydrogenation of ethylbenzene.

On the other hand,  $\text{N}_2\text{O}$  emission from nitric acid industry is one of the harmful gases to the environment, which causes the greenhouse effect and ozone layer depletion<sup>[9]</sup>. Besides, the activity of Fe-ZSM-5 in direct decomposition of  $\text{N}_2\text{O}$  has been studied for many years<sup>[10,11]</sup>. It is generally accepted that a  $\text{Fe}^{2+}$  ion forms the core of the catalytic site<sup>[12]</sup>. In this regard oxidation of  $\text{Fe}^{2+}$  ions by  $\text{N}_2\text{O}$  is suitable to transform  $\text{Fe}^{2+}$  ions to  $\text{Fe}^{3+}$  ions (equation 2). It should be noted that during  $\text{N}_2\text{O}$  catalytic decomposition the amount of  $\text{Fe}^{3+}$  ions increases, indicating that divalent iron is oxidized<sup>[13]</sup>.



More recently, it has been discovered that carbon dioxide could markedly promote the dehydrogenation of ethylbenzene over iron oxide catalysts through the reverse water–gas shift reaction (RWGS), which produces  $\text{H}_2\text{O}$  and  $\text{CO}$  [14,15] (equation 3).



Ikenaga et al. have reported the positive role of carbon dioxide as an oxidizing agent in the dehydrogenation of ethylbenzene. They demonstrated that the carbon dioxide could reduce the chromium oxide species and reoxidate them to chromium (III) oxide<sup>[16]</sup>.

Regarding the above mentioned points; in this study, the deactivation and regeneration of Fe-K commercial catalyst during the ethylbenzene dehydrogenation to styrene have been investigated. In addition, a method for regeneration of spent ethylbenzene dehydrogenation catalyst for reuse in this reaction has been presented. For this, a process for regenerating of ethylbenzene dehydrogenation catalyst comprises the steps of flushing with  $\text{N}_2\text{O}$  gas, passing steam containing  $\text{N}_2$  gas, flushing with air, passing oxygen-containing gas mixture comprising  $\text{N}_2\text{O}$  gas, and passing the mixture of  $\text{N}_2\text{O}$  and  $\text{CO}_2$  through used catalyst in the atmospheric pressure.

Furthermore, in the deactivation and regeneration process, phase changes and surface characteristics and also catalytic activity of fresh, used and regenerated catalysts for ethylbenzene dehydrogenation, were evaluated. The physicochemical properties of fresh, used and regenerated catalysts were examined using X-ray diffraction (XRD), scanning electron microscope (SEM),

BET measurement, ICP elemental analysis and hydrogen temperature-programmed reduction ( $\text{H}_2$ -TPR) techniques.

The decoking process and oxidation–reduction treatments for the deactivated catalyst have been examined for the purpose of regeneration of deactivated catalyst.

In addition, this research also presents the effective utilization of harmful and major greenhouse gases. A similar regeneration study has not yet been reported.

## EXPERIMENTAL

### Materials and regeneration procedures

The fresh commercial catalysts were obtained from BASF Company and ethylbenzene was obtained from the styrene monomer unit of Tabriz Petrochemical Company. The used catalysts were downloaded from an industrial reactor which had been used continuously under severe condition (LHSV =  $1 \text{ h}^{-1}$ ,  $T = 650 \text{ }^\circ\text{C}$ , mass ratio of steam to ethylbenzene = 1.3,  $P = 400\text{--}450 \text{ mmHg}$ ). The catalysts were in the form of cylindrical extrudate, with a diameter of 3 mm and length of 4–7 mm.  $\text{N}_2\text{O}$ ,  $\text{CO}_2$  and liquefied air were purchased from a commercial plant. For the steam generation high purity deionized water was used in the reaction. As shown in TABLE 1, activated catalysts as R1, R2, R3, R4 and R5 were prepared by passing different gaseous over used catalysts at  $660^\circ\text{C}$ .

### Catalyst characterization

The crystallinity of the all type of catalysts was checked by X-ray diffraction (D500 Siemens) using  $\text{Cu K}\alpha$  monochromatized radiation source (30–40 kV and 40–50 mA) in the range of  $2\theta = 4\text{--}70^\circ$ . The scanning electron microscope (SEM) images and microelemental analysis (EDX) are performed with Philips-XL30 equipped with a microanalysis system on samples coated with gold to decrease charging. BET surface area and total pore volume was measured by  $\text{N}_2$  adsorption-desorption isotherm at liquid nitrogen temperature using NOVA2000 (Quantachrome, USA). The chemical compositions of the catalysts were determined by an inductively coupled plasma spectrometer (ICP, GBC6-XL).  $\text{H}_2$ -TPR measurements were performed on catalysts pretreated in He flow (50 ml/min)

## Full Paper

**TABLE 1 : Different procedures for regeneration of used catalysts and physical properties of the fresh, used and regenerated catalysts**

Catalyst	Regeneration gas	Time (h)	$S_{\text{BET}}$ ( $\text{m}^2/\text{g}$ )	$V_p T \times 10^{-3}$ ( $\text{ml/g}$ )	$R_p A$ ( $\text{\AA}$ )
used	-	-	3.87	9.95	51.36
fresh	-	-	4.64	15.72	62.73
R1	air	11	6.79	10.15	29.9
R2	steam, $\text{N}_2$	11	2.13	4.13	38.88
R3	$\text{N}_2\text{O}$	11	1.75	6.24	71.36
R4	$\text{N}_2\text{O}$ , $\text{CO}_2$	9	5.25	7.75	29.53
R5	$\text{N}_2\text{O}$ , air	11	-	-	-

Note :  $S_{\text{BET}}$  (BET-surface area),  $V_p T$  (Total pore volume),  $R_p A$  (Average pore radius)

at 300°C for 1.5 h prior to heating under  $\text{H}_2$  flow (6 vol. % in Ar) from 20 to 900°C at a heating rate of 10°C.min<sup>-1</sup>.  $\text{H}_2$  consumption was continuously monitored by a thermal conductivity detector.

### Catalytic activity measurements

Catalytic experiments were carried out on commercial, used and activated catalysts, under atmospheric pressure in a continuous fixed-bed stainless steel reactor (i.d. 10 mm and length 500 mm) placed inside an electrically heated furnace. Prior to dehydrogenation of ethylbenzene, the reactor was loaded with 4.0 g of catalyst sample. The catalysts were activated at 660°C. It was carried out in a flow of  $\text{N}_2$  (100 ml/min) for 30 min and subsequently 1h in a flow of  $\text{H}_2\text{O}$  (14 ml.h<sup>-1</sup>). After the above mentioned pretreatments of the catalyst, the reaction was conducted for different catalysts.

Ethylbenzene was introduced by a pump with a feed rate of 30 mmol/h. Precise amounts of ethylbenzene, and other gaseous feed were mixed and introduced to a vaporization chamber at 250°C before being introduced to the catalytic reactor. A preheater was placed prior to reactor and allowed the stabilization of the composition of the gas mixture before each test. The catalytic tests were carried out for 1 h. Figure 1 shows a schematic diagram of used experimental set up. The outlet stream from the reactor was passed through a condenser and the products were collected for analysis. The reaction products were analyzed by a Shimadzu 2010 gas chromatograph apparatus with a flame inductivity detector (FID). Nitrogen was used as carrier gas, and flow rates were measured using a calibrated flow meter. For each measurement, at least three

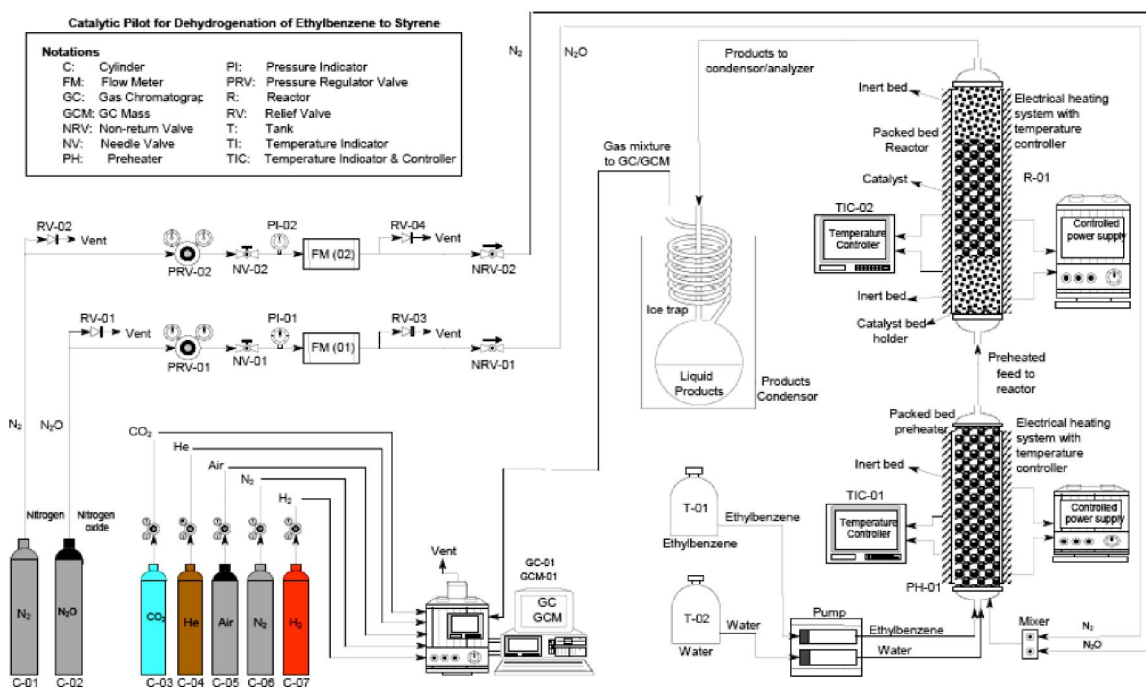


**Figure 1 : Schematic diagram of the experimental set up used for dehydrogenation of ethylbenzene to styrene**

repeated injections were taken, obtaining reproducible results. Air was used as a marker for the retention time correction, which was used to ensure the absence of dead volume when a new column was placed in the chromatograph. Styrene, toluene and benzene were the main desired products. When the test was to finish, the reactor was cooled by water until the temperature decreased to 250°C. A stream of nitrogen was finally

added until the reactor reached room temperature.

## RESULTS AND DISCUSSION

### X-ray diffraction

Since the type of iron oxide phases has the important effect on catalytic performance, therefore it is needed to identify different crystalline phases in

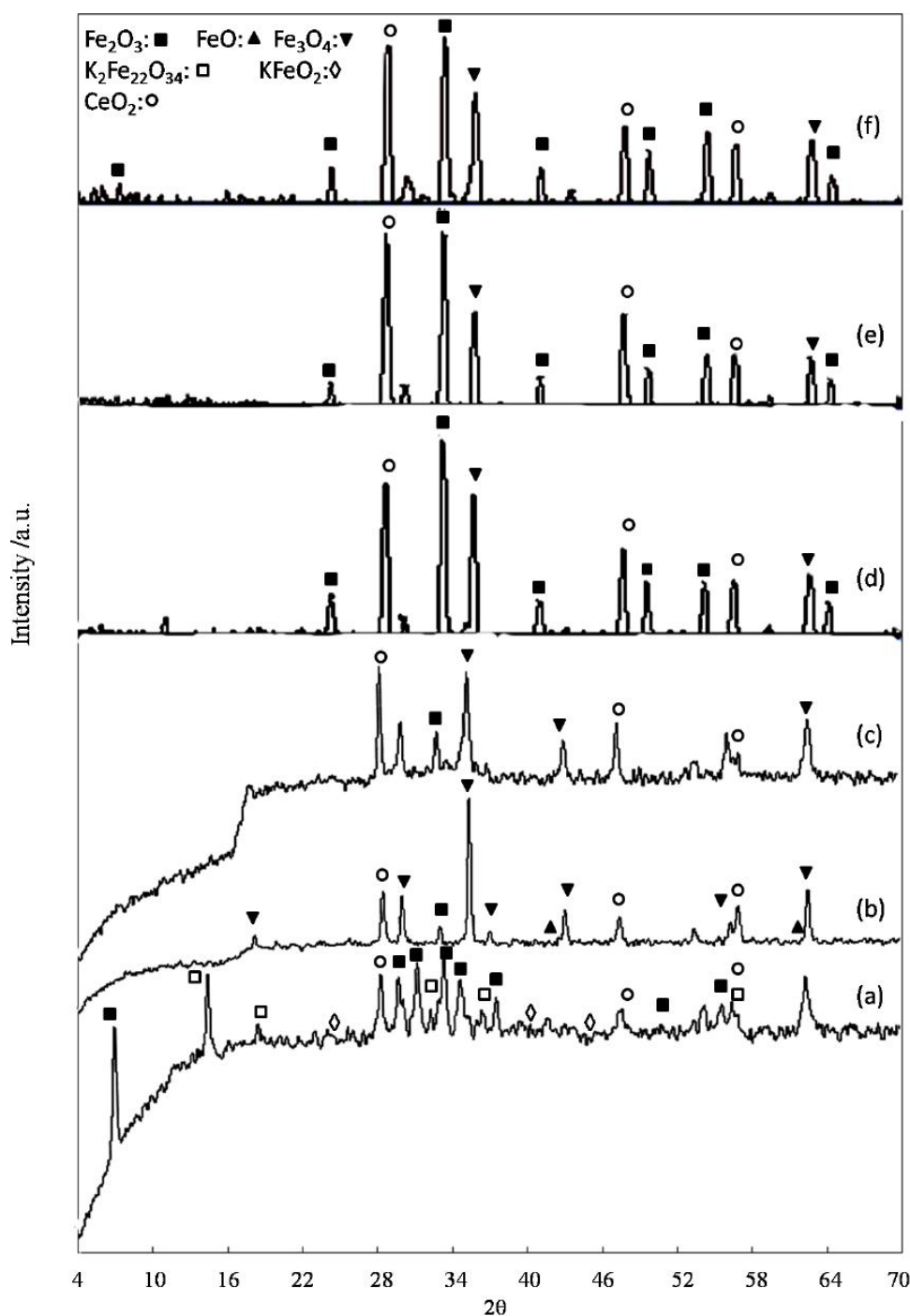


Figure 2 : X-ray powder diffraction patterns of (a): fresh, (b): used, (c): R2, (d): R1, (e): R3, (f): R5 catalysts



## Full Paper

ethylbenzene dehydrogenation catalysts. The iron oxide phases of catalysts were confirmed by means of the X-ray diffraction. The peaks at  $2\theta = 24.14^\circ, 33.15^\circ, 35.61^\circ, 40.85^\circ, 49.48^\circ, 54.09^\circ$  and  $63.99^\circ$  obtained in the diffractograms of the fresh sample can be well fitted to the data of the JCPDS card No. 33-0664 (hkl 012, 104, 113, 024, 116, 300), thus indicating the presence of hematite ( $\alpha\text{-Fe}_2\text{O}_3$ ). Also according to available data in JCPDS card No. 31-1034 peaks at  $2\theta = 8.62^\circ, 17.3^\circ, 35.0^\circ, 36.85^\circ, 39.49^\circ, 41.15^\circ, 44.2^\circ$  is related to the  $\text{K}_2\text{Fe}_{22}\text{O}_{34}$  phase. Therefore the Fe phase of fresh catalyst consists of the  $\text{Fe}_2\text{O}_3$ ,  $\text{K}_2\text{Fe}_{22}\text{O}_{34}$  and  $\text{KFeO}_2$  phases as can be seen in Figure (2: a).

XRD pattern of used sample shows that during the catalyst deactivation  $\text{Fe}_2\text{O}_3$ ,  $\text{K}_2\text{Fe}_{22}\text{O}_{34}$  and  $\text{KFeO}_2$  phases convert to  $\text{Fe}_3\text{O}_4$  and  $\text{FeO}$  phases. As illustrated in Figure 2 (b) existing peaks in the region  $2\theta = 30.16^\circ, 35.45^\circ, 43.25^\circ, 56.78^\circ, 62.72^\circ$  are related to the  $\text{Fe}_3\text{O}_4$  phase.  $\text{FeO}$  crystalline phase is catalytically inactive, and  $\text{Fe}_3\text{O}_4$  crystalline phase exhibits only a minor catalytic activity in the ethylbenzene dehydro-

genation reaction<sup>[1,6-8]</sup>.

These results suggest that the deactivation of the Fe-K commercial catalyst was due to change in iron bulk phase (i.e. the reduction of iron phase), which was proposed as a dominant factor of catalyst deactivation in the ethylbenzene dehydrogenation reaction<sup>[17]</sup>.

JCPDS card No. 43-1002 shows that the existing data in  $2\theta = 28.54^\circ, 47.48^\circ, 56.34^\circ$  is related to the  $\text{CeO}_2$  crystal phase which was observed in all fresh, used and activated samples, without any changes.

For the sample R3, as shown in Figure 2 (e), intensity of peaks related to the  $\text{Fe}_2\text{O}_3$  phase at  $2\theta = 24.14^\circ, 33.15^\circ, 40.85^\circ, 49.48^\circ, 54.09^\circ, 63.99^\circ$  has been increased and intensity of peaks related to  $\text{Fe}_3\text{O}_4$  crystalline phases has been reduced. Also all coke deposits in used catalyst in the presence of the  $\text{N}_2\text{O}$  were removed.

In R1 and R5 samples, peaks related to  $\text{Fe}_2\text{O}_3$  crystalline phase also observed but compared with the R3 catalyst, peaks have less intensity. It is worth to mention that coke deposition did not seen when  $\text{N}_2\text{O}$

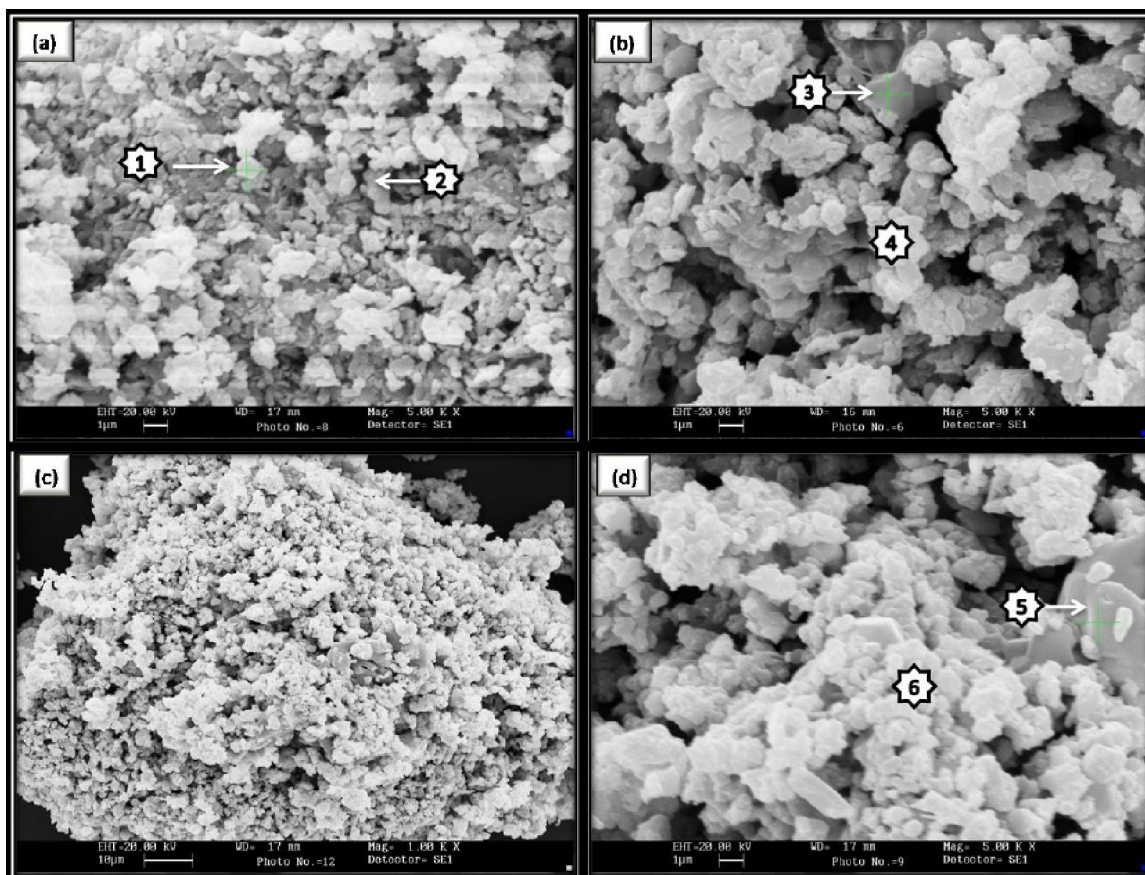


Figure 3 : SEM photographs of (a) fresh at 5000 $\times$  magnification, (b) U1 at 5000 $\times$  magnification and (c) U2 at 1000 $\times$  magnification (d) U2 at 5000 $\times$  magnification

gas was used. Thus can be resulted that  $N_2O$  gas can effectively eliminate coke deposits and increased  $Fe_2O_3$  crystalline phase.

### SEM images and specific surface area measurements

Surface area of the catalysts is one of the important factors for the reaction. As shown in TABLE 1, the BET surface areas,  $S_{BET}$ , are slightly decreased upon the deactivation compared with the fresh catalyst. A more pronounced decrease was seen in the BET-surface areas in the case of R2 and R3 catalysts.

In fact the BET surface area reduces when the catalyst deactivated by coking. It can be seen from these data that the average pore radius does affect the surface area and R3 with the highest average pore radius have the lowest surface area. Comparing the fresh and used catalyst samples, the surface area, total pore volume and pore radius are not almost the same. It indicates that the coke precursors deposited on the surface of the used catalyst block the pores of the catalyst.

In order to provide a deeper understanding of the possible causes of commercial catalysts deactivation, this section aims at studying the relationships between surface and structural features of the catalysts during its deactivation. These relationships were used to determine the causes of deactivation of the commercial catalysts during the styrene production by means of dehydrogenation of ethylbenzene with steam<sup>[18]</sup>.

The surfaces of the fresh, used and activated catalysts were characterized by SEM-EDX and are shown in Figures 3-6 and TABLE 2. Figure 3 (a) shows the

morphology of the surface of the fresh catalyst. As seen, agglomerates of 0.5–2  $\mu m$  particles were observed. Figures 3 (b-d) show SEM microphotographs of the outer layer and bulk of used catalyst (as U1 and U2, respectively) at various magnifications. These figures show that there are numerous dark grains on the surface and bulk of the used catalyst. TABLE 2 shows the chemical composition of different areas of Figures 3-6, as determined by EDX analysis.

EDX results show that the concentration of potassium species at the surface of the fresh catalyst is somewhat lower than in the bulk. Amount of potassium in the large dark particle is much higher than its surrounding material.

Figures 4 a and b show the SEM images of outer layer and bulk composition of R5 catalysts respectively. The dark particles could not be seen in these figures and EDX analysis confirmed that potassium and cerium species are much higher in the bulk than at the surface. Radial view of fresh and used catalysts in the Figures 5 a-d shows that unlike the used catalyst, dark and large particles could not be seen in the fresh catalyst. Thus we conclude that during the catalyst deactivation potassium concentrates in some dial large aggregates. This can be also one of the major causes of commercial catalyst deactivation.

It may be concluded from the radial view and EDX analysis that fresh and regenerated R5 catalysts have an essentially constant iron concentration.

### ICP analysis

The chemical compositions of the fresh and used catalysts (Fe, K, Cr, Mg, Ca and Mo) were determined by

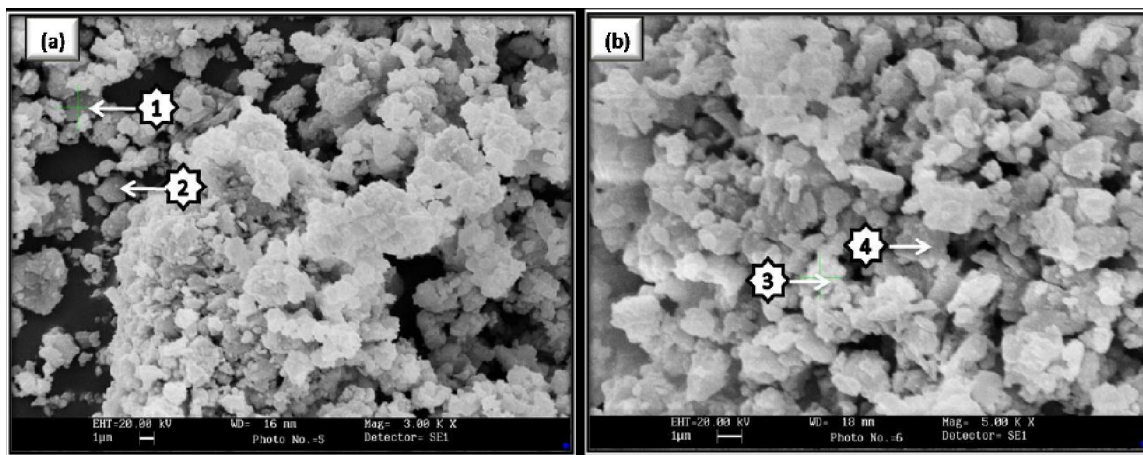


Figure 4 : SEM photographs of (a) R5-1 at 3000 $\times$  magnification and (b) R5-2 at 5000 $\times$  magnification



## Full Paper

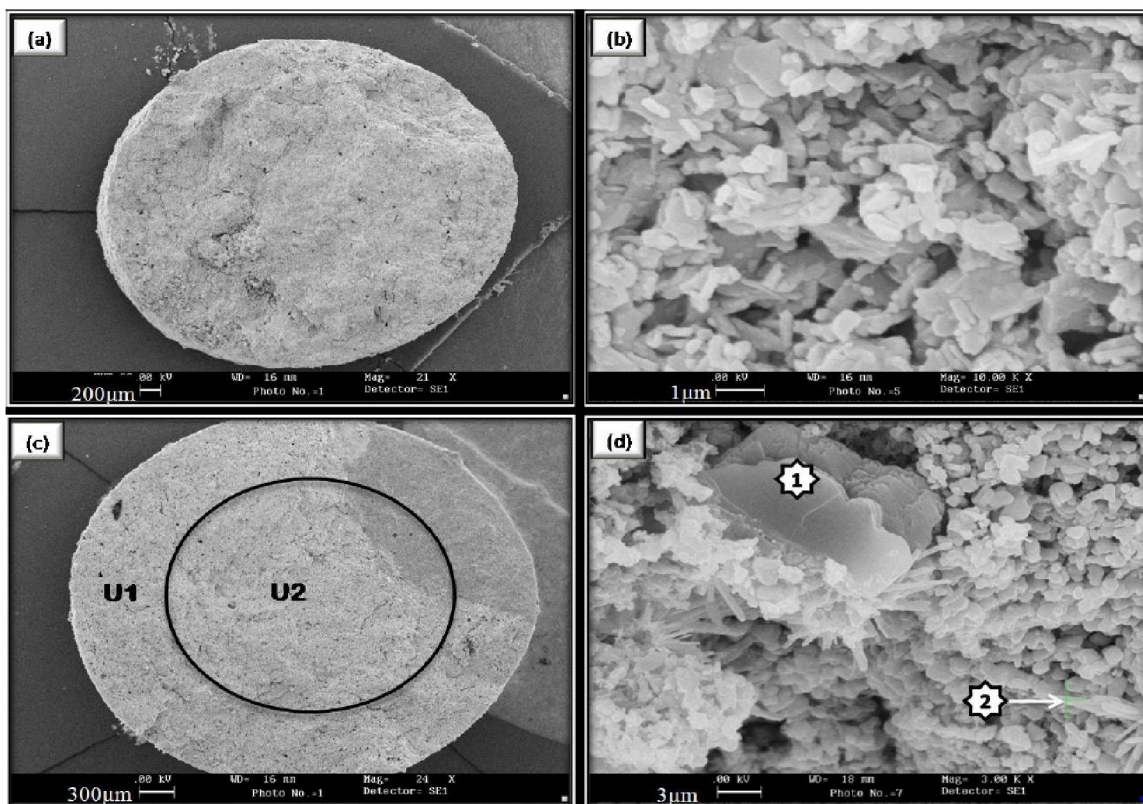


Figure 5 : SEM photographs of (a, b) radial view of fresh catalysts at 21 $\times$  and 10000 $\times$  magnification, respectively and (c, d) radial view of used catalysts at 24 $\times$  and 3000 $\times$  magnification, respectively

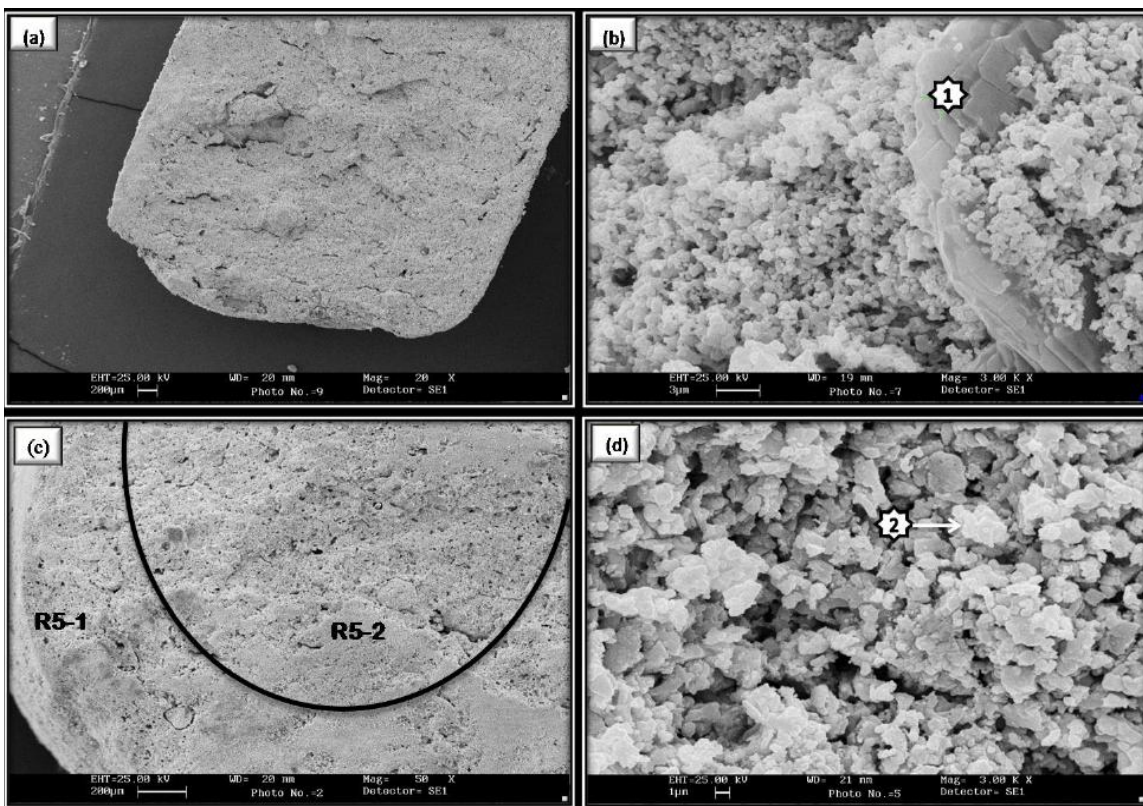


Figure 6 : SEM photographs of (a, b) axial view of used catalysts at 20 $\times$  and 3000 $\times$  magnification, respectively and (c, d) radial view of R5 catalysts at 50 $\times$  and 3000 $\times$  magnification, respectively

an inductively coupled plasma spectrometer. Comparison of analysis of fresh and used catalysts in TABLE 3 shows that the concentration of potassium in spent catalyst had decreased more than 27%. The amount of other species such as Mg and Ca ions remained practically unchanged after using the catalyst. Furthermore, it is found that the increase of Cr/Fe ratio of the used catalyst is negligible, indicating that there is almost no loss for chrome species during the deactivation. The slight increase is due to losses of other species.

### Temperature-programmed reduction

The stability of framework Fe(III) and Fe(II) species in the fresh, used and regenerated catalysts towards reduction could be further confirmed by H<sub>2</sub>-TPR. Reduction (TPR) profiles of the catalyst samples are shown in figures 7 and 8. As shown in table 4, three main H<sub>2</sub> consumption peaks can be discriminated: i) less than 400°C ii) between 400 and 600°C, and iii) above

600°C.

As shown in Figure 7 (a) the fresh sample displayed two peaks at 563 and 710 °C. According to literatures<sup>[19-21]</sup> the first one is assigned to the reduction of Fe<sub>2</sub>O<sub>3</sub> to FeO while the broad peak at high temperature is related to the reduction of FeO to Fe. TPR analysis of used catalyst (Figure 7: b) suggested that the signals appeared at 482 and 804°C are related to the reduction of hematite ( $\alpha$ -Fe<sub>2</sub>O<sub>3</sub>) to magnetite (Fe<sub>3</sub>O<sub>4</sub>) and reduction of magnetite to produce metallic iron, respectively<sup>[22]</sup>. It can be noted that, the used catalyst reduction peak of Fe<sub>2</sub>O<sub>3</sub> to FeO shifts to low temperature, i.e. from 563 to 482°C. Perhaps a large amount of cokes in the used sample catalyzes the reduction of iron (III) oxide. The lower intensity of the Fe<sub>2</sub>O<sub>3</sub> reduction peak for used catalyst compared to fresh catalyst suggests that a lower Fe(III) species is achievable.

Compared with the fresh catalyst a very similar reduction profile was obtained for the R1 catalyst, and

**TABLE 2 : Total and point chemical composition (atomic. %) of fresh, used and regenerated catalysts, performed by EDX analysis**

Catalyst	Area of EDX analysis	Fe (Atomic %)	K (Atomic %)	Cr (Atomic %)	Ce (Atomic %)	Mg (Atomic %)	Ca (Atomic %)
fresh	1	76.64	18.09	-	2.84	-	2.43
	2	76.77	11.2	-	3.43	7.12	1.38
	3	70.96	23.78	1.06	4.21	-	-
used -1	4	86.13	2.90	1.31	5.4	4.26	-
	5	38.46	49.3	4.35	3.97	-	3.92
used -2	6	83.75	8.25	1.45	5.66	0.89	-
	1	91.28	1.2	1.17	4.77	-	1.57
R5-1	2	93.63	4.86	-	-	1.33	0.19
	3	82.76	6.51	1.25	8.17	-	1.31
R5-2	4	84.08	5.27	1.72	6.58	-	0.47
	Total	81.03	7.31	-	2.22	4.26	5.18
Fresh (radial)	1	65.57	30.72	-	3.71	-	-
	2	85.67	-	0.97	-	-	13.35
used (radial)	1	68.65	27.79	-	2.86	-	0.7
	Total	84.82	6.38	-	5.1	-	3.69
R5 (radial)	2	91.4	3	0.17	1.71	-	3.72

**TABLE 3 : Chemical composition (mg/l and wt. %) of fresh and used catalysts, performed by ICP analysis**

Catalyst	Amount of elements	Fe	K	Cr	Mg	Ca	Mo
Fresh	(mg/l)	423.6	55	0.14	9.4	14.8	17.2
	(wt.%)	81.44	10.57	0.02	1.8	2.84	3.3
Used	(mg/l)	450.4	40	0.26	9.4	13	9.3
	(wt.%)	86.2	7.65	0.05	1.8	2.48	1.78



## Full Paper

compared with the used catalyst the high stability of framework Fe(III) in R1 towards reduction could be confirmed by H<sub>2</sub>-TPR, as presented in Figure 7 (c).

In the R2 and R4 catalysts three peaks were observed (Figures 8: a and c). Such a profile, apparently more complex than typical fresh catalyst, reflects the presence of not only the two different iron species but also of other phases, all undergoing reduction in the same temperature range, thus leading to a probable peak overlapping.

In the R3 catalyst the broad peak at 849°C was associated with the peak observed at 592°C and corresponds to the second reduction step (Fe<sup>2+</sup>→Fe<sup>0</sup>).

For the R2 and R3 catalysts the last peak that is observed at a very high temperature (about 850 °C) is

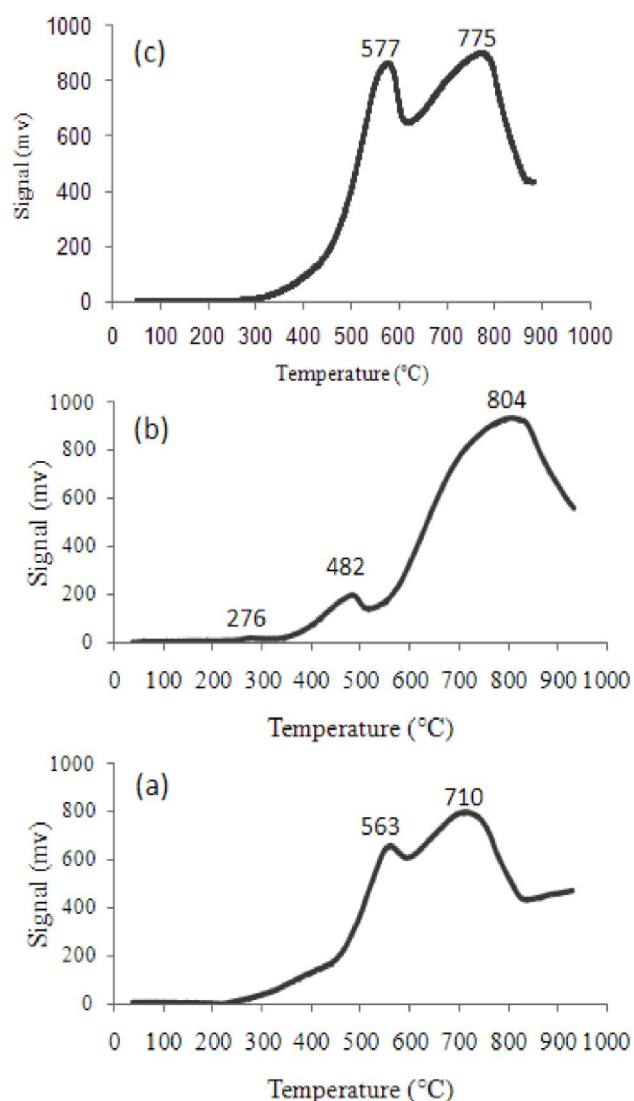


Figure 7 : Temperature-programmed reduction curves of the (a) fresh, (b) used and (c) R1 catalysts

very intense and should be related to stable and hardly reducible Fe<sup>2+</sup> species present in the steam and N<sub>2</sub>O regenerated catalysts.

Also as shown in Figures 7 and 8 one sharp reduction peak was observed for all catalysts, revealed that the reduction of Fe(III) species was complete and ended with the formation of Fe(0).

As shown in figure (8: b) since the Fe<sup>3+</sup> species are the active sites for the ethylbenzene dehydrogenation reaction<sup>[23,24]</sup>, the TPR profiles of R3 catalyst suggest that catalyst regeneration with N<sub>2</sub>O feed can delay the reduction of Fe<sup>3+</sup> species and deactivation process during the catalytic test.

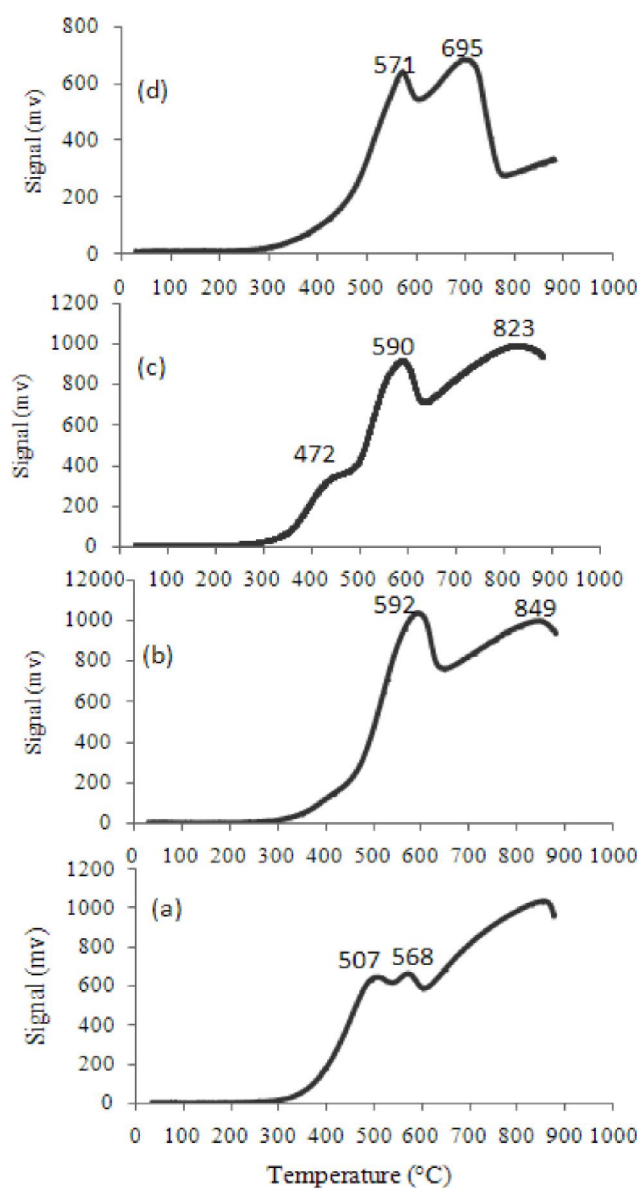
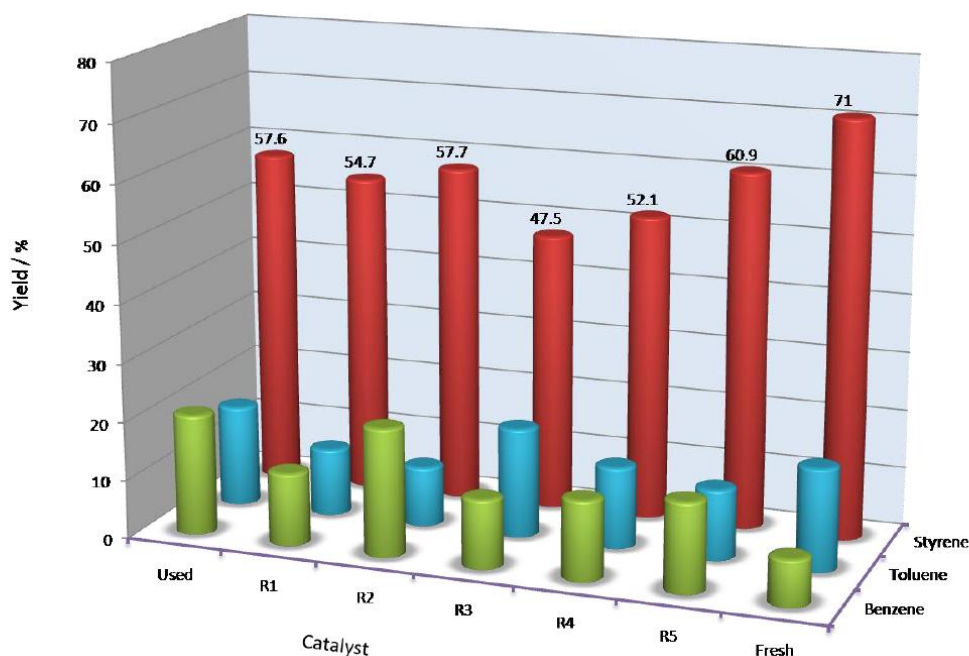


Figure 8 : Temperature-programmed reduction curves of the (a) R2, (b) R3, (c) R4 and (d) R5 catalysts

TABLE 4 : Amounts of hydrogen consumption during H<sub>2</sub>-TPR measurements for catalysts

Catalyst	Peak Temperature (°C)			Amount of H <sub>2</sub> Consumption (cc/g)			Total (cc/g)
	I	II	III	I (less than 400°C)	II (400-600°C)	III (600-1000°C)	
U	276	482	804	0.08	1.56	37.8	39.44
F	-	563	710	-	3.76	13.9	17.66
R1	-	577	775	-	1.5	19.7	21.2
R2	-	507	-	-	3.4	-	4.05
		568			0.65		
R3	-	592	849	-	1.9	4.14	6.04
R4	-	472	823	-	0.19	4.2	11.51
		590			7.12		
R5	-	571	695	-	7	16	23

Figure 9 : Yield of styrene, toluene and benzene for fresh, used and regenerated catalysts in dehydrogenation of ethylbenzene in the presence of steam (H<sub>2</sub>O/EB=4.4, WHSV=0.9 h<sup>-1</sup>) at 660 °C

### Catalytic tests

In order to investigate the relationship between the regenerating gas and activity of regenerated catalysts, the performance of fresh, used and regenerated catalysts in the ethylbenzene dehydrogenation reactions is compared at 660°C with applying a ratio of H<sub>2</sub>O/EB=4.4 and WHSV=0.9 h<sup>-1</sup> at the atmospheric pressure. The results of catalytic tests are shown in Figure 9. Through a long-term deactivation, used catalyst showed significant decrease in the styrene yield but the yield of benzene, which is an undesired product, increases and is the highest for used R2 catalyst. Maximum yield of toluene, as by-product related to R3 catalyst as a regenerated catalyst, which is equal to 23.9%.

The best performance was observed over R5 catalyst, which is an additional feature of regenerate catalyst with N<sub>2</sub>O. These results clearly show that regeneration with N<sub>2</sub>O activates the used catalyst most likely by formation of Fe<sup>3+</sup> species.

For comparison, the results are also included in TABLE 5. The styrene selectivity increases as the coke is removed, indicating that all regeneration procedures have a significant effect on the dehydrogenation activity of the regenerated catalysts. It will be understood from TABLE 5 that, used catalyst has highest conversion but produces higher amount of benzene and toluene by-products, which reduce the styrene yield and selectivity. However, it was also observed that regenerated R5 catalyst has the highest ethylbenzene conversion among

## Full Paper

all activated catalysts and activity of fresh catalyst is a little more than that of this catalyst. The steady state selectivity toward styrene for the catalysts is in the order of: fresh >R1>R4>R5>R2>R3> used.

**TABLE 5 : The performance of fresh, used and regenerated catalysts for the dehydrogenation of ethylbenzene in the presence of steam**

Catalyst	Temperature (°C)	WHSV (h <sup>-1</sup> )	H <sub>2</sub> O/EB (cc/cc)	Ethylbenzene conversion (%)	Styrene selectivity (%)
U	660	0.9	4.4	97.3	59.1
F	660	0.9	4.4	96.5	73.5
R1	660	0.9	4.4	81.7	67
R2	660	0.9	4.4	89.9	64.2
R3	660	0.9	4.4	78.2	60.7
R4	660	0.9	4.4	79.6	65.4
R5	660	0.9	4.4	94.5	64.4

## CONCLUSION

This study generally demonstrates a novel process for regeneration of catalysts used in dehydrogenation of ethylbenzene. Used catalysts were activated with oxidants like N<sub>2</sub>O, CO<sub>2</sub>, air, steam and mixtures of these components. The catalyst characterization has been carried out to gain insight into the catalyst deactivation

N<sub>2</sub>O was found to be very useful to enhance the oxidation state of Fe<sup>2+</sup> species, as confirmed by the XRD and TPR experiments. Furthermore, N<sub>2</sub>O can effectively eliminate coke deposits and increase Fe<sub>2</sub>O<sub>3</sub> crystalline phase. It is also found that BET surface area, particle size and crystalline phases of the catalysts influenced by regeneration method.

Ethylbenzene dehydrogenation reactions were carried out at 660°C over various regenerated catalysts. N<sub>2</sub>O was demonstrated to be highly active for regeneration of used catalyst and the best results were obtained over R5 catalyst at 660°C with a conversion of 94.5% and styrene yield of 60.9%.

## ACKNOWLEDGMENTS

The authors would like to thank the University of Tabriz and Iranian Petrochemical Research and Technology Company for the financial support of this project.

## REFERENCES

[1] G.R.Meima, P.G.Menon; *Appl.Catal.A*, **212**, 239-245 (2001).

- [2] W.D.Mross; *Catal.Rev.Sci.Eng.*, **25**, 591-637 (1983).
- [3] F.Cavani, F.Trifiro; *Appl.Catal.A*, **133**, 219-239 (1995).
- [4] N.Dulamiță, A.Măicăneanu, D.C.Sayle, M.Stanca, R.Crăciun, M.Olea, C.Afloroaei, A.Fodor; *Appl.Catal.A*, **287**, 9-18 (2005).
- [5] I.Rossetti, E.Bencini, L.Trentini, L.Forni; *Appl.Catal.A*, **292**, 118-123 (2005).
- [6] Y.Joseph, C.Kuhrs, W.Ranke, M.Ritter, W.Weiss; *Chem.Phys.Lett.*, **314**, 195-202 (1999).
- [7] Y.Joseph, M.Wuhn, A.Niklewski, W.Ranke, W.Weiss, C.Woll, R.Schlogla; *Phys.Chem.Chem.Phys.*, **2**, 5314-5319 (2000).
- [8] O.Shekhah, W.Ranke, R.Schlogl; *J.Catal.*, **225**, 56-68 (2004).
- [9] P.Kuśtrowski, L.Chmielarz, A.Rafalska-Łasocho, B.Dudek, A.Pattek-Janczyk, R.Dziembaj; *Catal.Comm.*, **7**, 1047-1052 (2006).
- [10] E.Berrier, O.Ovsitser, E.V.Kondratenko, M.Schwider, W.Grünert, A.Brückner; *J.Catal.*, **249**, 67-78 (2007).
- [11] M.Santhosh Kumar, J.Pérez-Ramírez, M.N.Debbagh, B.Smarsly, A.Brückner; *Appl.Catal.B*, **62**, 244-254 (2006).
- [12] G.I.Panov, G.A.Sheveleva, A.S.Kharitonov, V.N.Romannikov, L.A.Vostrikova; *Appl.Catal.A*, **82**, 31-36 (1992).
- [13] P.K.Roy, R.Prins, G.D.Pirngruber; *Appl.Catal.B*, **80**, 226-236 (2008).
- [14] K.N.Rao, B.M.Reddy, B.Abhishek, Y.H.Seo, N.Jiang, S.E.Park; *Appl.Catal.B*, **91**, 649-656 (2009).
- [15] T.P.Braga, A.N.Pinheiro, C.V.Teixeira, A.Valentini; *Appl.Catal.A*, **366**, 193-200 (2009).
- [16] N.O.Ikenga, T.Tsuruda, K.Senma, T.Yamaguchi,



- Y.Sakurai, T.Suzuki; *Ind.Eng.Chem.Res.*, **39**, 1228-1234 (2000).
- [17] W.Weiss, W.Ranke; *Prog.Surf.Sci.*, **70**, 1-151 (2002).
- [18] R.M.Freire, F.F.de Sousa, A.L.Pinheiro, E.Longhinotti, J.M.Filho, A.C.Oliveira, P.T.C.Freire, A.P. Ayala, A.C.Oliveira; *Appl.Catal.A*, **359**, 165-179 (2009).
- [19] R.Furuichi, M.Hachia, T.Ishii; *Thermochim.Acta.*, **133**, 101-106 (1988).
- [20] H.Lin, Y.Chen, C.Li; *Thermochim.Acta.*, **400**, 61-67 (2003).
- [21] E.Rombi, I.Ferino, R.Monaci, C.Picciau, V.Solinas, R.Buzzoni; *Appl.Catal.A*, **266**, 73-79 (2004).
- [22] M.S.Santos, S.G.Marchetti, A.Albornoz, M.C.Rangel; *Catal.Today*, **133-135**, 160-167 (2008).
- [23] M.S.Ramos, M.S.Santos, L.P.Gomes, A.Albornoz, M.C.Rangel; *Appl.Catal.A*, **341**, 12-17 (2008).
- [24] B.D.Herzog, H.F.Raso; *Ind.Eng.Chem.Prod.Res.Dev.*, **23**, 187-196 (1984).